RSC Advances

ROYAL SOCIETY OF CHEMISTRY

www.rsc.org/advances

RSC Advances

ARTICLE

Platycodin D inhibits B16F10 melanoma metastasis via antiangiogenic activity

Received 00th January 20xx,
Accepted 00th January 20xx

DOI: 10.1039/x0xx00000x

www.rsc.org/

Siwen Zheng [a], Wei Li [a, b], Jia Wang [a], Yinbin Chen [a], Wei Hou [a], Wei Gao [a], Qingxiu Liu [a, b], Yingping Wang [a]*

Platycodin D (PD) was an active component that is mainly isolated from the roots of Platycodon grandiflorum, and it has been suggested to exhibit anticancer activities. In this study, anti-B16F10 melanoma metastasis activities of PD and related antimetastasis mechanisms were investigated *in vitro* and *in vivo*. *In vitro*, PD altered the cytoskeleton of B16F10 cells and inhibited B16F10 cell viability, as well as cell adhesion on human umbilical vein endothelial cells (HUVECs), cell migration, cell invasion. Moreover, PD inhibited the ability of HUVECs proliferation and tube formation. Further more, PD exhibits non-toxic and good biocompatibility under certain concentration(20 μg/mL). *In vivo*, PD (3 and 6 mg/kg) inhibited B16F10 cells lung metastasis and tumour angiogenesis in an experimental lung metastasis mouse model. In addition, PD significantly decreased the levels of matrix metalloproteinases (MMPs) and increased the serum levels of cytokines includinginterleukin-12 (IL-12), tumour necrosis factor-α (TNF-α), and interferon-γ (IFN-γ) in experimental mice. Taken together, these results clearly indicated that PD inhibited B16F10 melanoma metastasis via antiangiogenic activity.

1 Introduction

Melanoma is a malignant cancer that originates from melanocytes, specialised pigmented cells found in the epidermis.[1] As the most aggressive form of skin cancer, the incidence of melanoma is increasing worldwide, and it is also a frequent cancer found in adolescents and young adults. Among cancers in patients under 40 years of age, the incidence of melanoma is highest for males and second highest only to that of breast cancer for females. It is also one of the most difficult cancers to treat[2, 3], and detection of the highest risk of metastasis primary tumours is challenging.[4] B16F10 is one of the B16 melanoma sublines, that demonstrates highly metastatic characteristics, and it preferentially metastasises to the lung following intravenous injection.[5]

Tumour metastasis is malignant cells spread from the primary site to a remote location. It consists of a series of complicated processes, including a loss of adhesion between cells and the proteolytic degradation of the extracellular matrix (ECM), entrance into the bloodstream and arrest in circulation, invasion into new organs and subsequent growth.[6] This concerning growth is the most harmful aspect of cancer.[7] Angiogenesis is necessary for aggressive tumour growth and metastasis.[8, 9] Avascular tumours are severely restricted in their growth potential because of the lack of a blood supply. For tumours to develop in size and metastatic potential they must make an "angiogenic switch" through perturbing the local balance of proangiogenic and antiangiogenic factors. Thus, angiogenesis is a key point in the control of cancer progression. Its inhibition represents a significant new approach to further improve antiangiogenic and anticancer activity.[10-12]

Modern medicine to cure cancer is highly hydrophobic (poor bioavailability) and shows a lack of specificity to particular tumour sites, causing severe toxicity to normal tissues and organs.[13] For example, cisplatin is an anticancer clinical drug, and its toxic side effects for kidney and other organ has been confirmed.[14] Natural products are safe and exhibit little side effects. It also has better effects and lower cost in treatment. Thus, natural products have received increasing attention in cancer treatment.[15-17] These compounds can be clinically used on their own or in combination with other natural products or drugs.[18] Until recently, several species of natural compounds have proven their therapeutic potential in melanoma metastasis, including alkaloids, polyphenols, vitamin-related compounds, terpenoids, peptides and herbal extracts. [19]

Platycodin D (PD, Figure 1) is a triterpenoid saponin isolated from the roots of *Platycodon grandiflorum.*[20] It possesses multiple pharmacological activities including liver protection,[21] anti-obesity,[22] anti-rheumatoid arthritis,[23] anti-inflammatory,[24] anti-nociceptive,[25] immunomodulatory,[26] anti-atherosclerosis,[27] and anticancer properties. The various anticancer activities can induce apoptosis and inhibit proliferation, migration, invasion or xenograft growth of human tumour cell lines, including hepatic,[28,29] pulmonary,[30] ovarian[31], gastric,[32] glioma,[33] leukaemia,[34,35] and breast[36,37] cancer cells, etc. Li *et al.*[38] has reported that PD triggered autophagy in a series of cancer cell lines and Luan *et al.*[20] has demonstrated that PD can significantly inhibit the growth of HCT-15 xenografts in mice. Moreover, it decreased tumour microvessel

[a] *Institute of Special Animal and Plant Sciences of Chinese Academy of Agricultural Sciences, Changchun, 130112, China. E-mail: yingpingw@yeah.net ; Tel: +86-431-81919856.*
[b] *College of Chinese Medicinal Materials, Jilin Agricultural University, Changchun, 130118, China.*

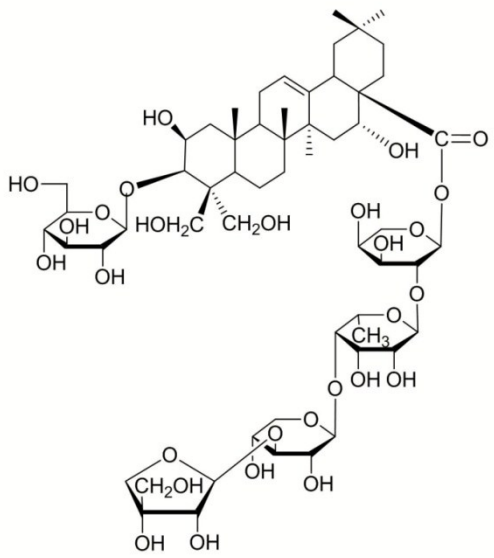

Fig.1 Chemical structure of PD.

density (MVD), a related mechanism of PD-mediated antiangiogenic activity via the suppression of the activation of vascular endothelial growth factor receptor 2 (VEGFR2)-mediated signalling pathway. Chun *et al.*[39] found that PD inhibited MDA-MB-231 human breast cancer cells migration, invasion and the growth of MDA-MB-231 xenograft tumours in BALB/c nude mice. The mechanisms of action exerted by PD involved the down-regulation of EGFR and the inhibition of EGF-induced activation of the EGFR, MAPK, and PI3K/Akt pathways. Taken together, these reports suggested that the ability of PD to suppress on tumour growth and metastasis was associated with a tumour angiogenesis factor. Interestingly, PD exhibits potential cytotoxicity in several cancer cell lines *in vitro* and inhibits the effect on a carcinoma transplant solid tumour model *in vivo*. However, thus far, information regarding the anti-tumour metastasis and angiogenesis of PD *in vivo* is relatively limited. Given the anti-tumour metastasis effect of PD on B16F10 melanoma *in vivo* and *in vitro*, the present study was designed to investigate the suppressive efficacy of PD in an experimental lung metastasis mouse model and several cell models. This study aimed conducted to demonstrate the anti-tumour metastasis activity of PD in a B16F10 melanoma lung metastasis model and its potential tumour angiogenesis molecular mechanism.

2 Materials and methods

2.1 Reagents, cell lines and animals

PD (Purity > 98%)was purified from the methanol extract of *Platycodon grandiflorum* as described in our previous paper.[40] Foetal bovine serum (FBS) was purchased from Gibco (BRL Co. Ltd.USA), 3-(4,5-Dimethylthiazol-2-yl)-2, 5-diphenyltetrazolium bromide (MTT) was purchased from Sigma (St. Louis, MO), actin tracker green staining solution was obtained from Beyotime Institute of Biotechnology (Nanjing, China). The Elisa kit was purchased from R&D Systems (Minneapolis, MN, USA).

B16F10 melanoma cell lines and human umbilical vein endothelial cells (HUVECs) were purchased from the Type Culture Collection of the Chinese Academy of Sciences (Shanghai, China). The cells were cultured in DMEM, containing 10% FBS (v/v), supplemented with penicillin and streptomycin routinely. Both B16F10 and HUVECs were cultured at 37°C in a humidified atmosphere containing 5% carbon dioxide (CO_2).

Male C57BL/6J mice (6 - 8 weeks old) were purchased from Vital River Laboratories (Beijing, China). Male SD mice (8 weeks old) were purchased from Changchun Institute of Biological Products Co. Ltd. (Changchun, China). Throughout the experiments, mice were maintained in plastic cages on a 12h light/dark cycle and access to food and water was *ad libitum*. Animal welfare and experimental procedures were performed strictly in accordance with the care and use of laboratory animals. The experiments were performed according to the Guide for the Care and Use of Laboratory Animals (Ministry of Science and Technology of China, 2006). All experimental procedures were approved by the Ethical Committee for Laboratory Animals of Institute of Special Animal and Plant Sciences of Chinese Academy of Agricultural Sciences, Changchun 130112, China.

2.2 Cell viability assay

In this study, PD was dissolved in dimethyl sulfoxide (DMSO) and diluted in DMEM, and then filtered using a 0.22-μm membrane. The effect of PD on B16F10 and HUVEC cell growth was performed using the MTT assay.[41] Briefly, exponentially growing B16F10 (1×10^4 cells/well) and HUVEC (7×10^3 cells/well) cells were seeded onto 96-well plates and incubated for 24 h in complete medium. After 24 h incubation, the cells were treated with various concentrations of PD (0, 5, 10, 20, 40, 80 μg/mL for B16F10 and 0, 5, 10, 20, 40, μg/mL for HUVECs) for 24h, and MTT (0.5%, 20 μL) was then added to each well and incubated for an additional 4 h at 37°C. The formazan crystals were dissolved in DMSO (150 μL), and the absorbance at 490 nm was measured using a microplate reader (BioTek Epoch, BioTek, Winooski, VT, USA)

2.3 Measurement of cell adhesion

A sensitive ELISA method based on the cellular uptake of Rose-Bengal stain was used to measure the effect of PD on the adhesion of B16F10 and human umbilical vein endothelial cells (HUVECs).[42] Briefly, HUVEC cells were seeded onto a 96-well plate and grown in 37°C for 24 h to form a monolayer of cells. The cells were then washed with DMEM containing 10% FBS. B16F10 cells suspension(5×10^4 cells/well, 200 μL) with or without PD (0, 5,10, 20 and 40 μg/mL) was added to the HUVECs and incubated at 37°C for 30min in a 5% CO_2 incubator. Non-adherent cells were removed by DMEM medium. Next, 0.25% Rose-Bengal (100 μL/well) was added and incubated for 5 min at room temperature. The stain was removed and the wells were washed twice with DMEM containing 10% FBS. A solution of ethanol and PBS (1:1) was used to treat the 96-well plate for 30 min to release the stain. The optical density at 570 nm for each well was determined using an ELISA reader (BioTek Epoch, BioTek, Winooski, VT, USA).

2.4 Morphological characteristics of B16F10 cells

Sulforhodamine B staining assay was performed for further morphological observation of B16F10 cells. Briefly, cells were washed by PBS after PD treatment and fixed with 4% paraformaldehyde, and then stained with the sulforhodamine B for 20 min. After the cells were washed by 1% acetic acid, the cells were imaged under an inverted microscope. (Nikon eclipse Ti, Nikon, Tokyo, Japan).

The filamentous actin (F-actin) cytoskeleton is a dynamic structure that is necessary for the regulation of cell motility. FITC-labelled phalloidin was used to detect the distribution of actin filaments.[43] To assess the effect of PD on the cell cytoskeleton, B16F10 cells were seeded onto 24-well plates and incubated for 24h. After the PD (0, 5, 10, 20 and 40 μg/mL) solution was added to the plates, all of the cells were further incubated at 37 °C for 24 h. Next, the cells were rinsed with PBS, and the cells were fixed with 3.7% paraformaldehyde and permeabilised in 0.1% Triton X-100 in PBS for 10 min. Phalloidin conjugated to FITC in a solution containing 0.1% Triton X-100 in PBS and 5% BSA was added to stain F-actin. After incubation for 60 min at room temperature, the cells were extensively washed to reduce nonspecific interactions. The nuclei of the cells were stained by DAPI. The cells were imaged using a fluorescence microscope (Nikon eclipse Ti, Nikon, Tokyo, Japan).

2.5 Cell migration assay

The wound healing migration assay was performed as previous described.[44] B16F10 cells were seeded in a 6-well plate and incubated for 24 h, wounding was performed by scraping through the monolayer of cells with a 200 μL pipette tip. Cells were washed twice with phosphate-buffered saline (PBS) to remove cell debris, and then incubated with different concentrations (0, 5, 10, 20 and 40 μg/mL) of PD for 24 h. The wound was imaged at 0 and 24 h under an inverted microscope. (Nikon eclipse Ti, Nikon, Tokyo, Japan). Image analysis was performed using Image-ProPlus 6.0 software.

2.6 Cell invasion assay

The B16F10 cells invasion assay was performed using transwell chambers as previously described.[45] Serum-free DMEM diluted matrigel matrix (50 μg/well) was placed in the upper chamber of the transwell chamber (pore size of 8 μm), and incubated for 2 h at37°C in a carbon dioxide incubator for gelling. B16F10 cells (5 × 10^4 cells/well) were seeded on the upper chamber in DMEM containing 2% FBS and the concentration of PD was 0, 5, 10, 20 and 40 μg/mL. A solution of 10% FBS in DMEM was placed in the lower well. The cells were incubated at 37°C for 24 h. Non-invasive cells on the upper surface of the membrane were removed by wiping with cotton swabs. The cells that invaded the underside of the insert membrane were fixed with 4% paraformaldehyde and stained with crystal violet. The migrated cells were observed and quantified under a microscope (Nikon eclipse Ti, Nikon, Tokyo, Japan).

2.7 Tube formation assay

The tube formation assay was performed as previously described.[46] Matrigel (BD Biosciences, San Jose, CA) was thawed overnight at 4°C. Next, 50 μL matrigel was coated to the pre-chilled 96-well plates per well, and then incubated at 37°C for 1h. HUVECs (5 × 10^4 cells/well) were seeded on the matrigel and treated with various concentrations of PD (0, 5, 10, 20 and 40 μg/mL). After incubation for 5 h, the formation of HUVECs tubular structures was captured using a microscope (Nikon eclipse Ti, Nikon, Tokyo, Japan). The tube length was quantified using Image-ProPlus 6.0 software.

2.8 Haemolysis test

To evaluate the haemocompatibility of PD, the haemolysis test was performed as previously described with some modifications.[47] Arterial blood was obtained from healthy SD mice and erythrocytes were separated from the plasma and lymphocytes by centrifugation (3000 r/min, 5 min) at 4°C, washed three times with normal saline and suspended in normal physiological saline at a haematocrit of 2%. Erythrocytes were used immediately after isolation. Next, 2.5 ml erythrocyte suspension and 2.5 ml medicated saline solution were added to a 10-ml centrifuge tube. The final concentration of PD was 5, 10, 20, 40 μg/mL, respectively. The negative and positive controls were normal physiological saline and 0.2% Triton X-100. The samples were incubated for a specific time period at 37 °C for 60 min. Next, the tube was centrifuged at 3000 r/min for 5 min. Finally, the optical density (OD) was obtained at a wavelength of 545 nm. Three paralleled samples were laid in each group. The mean value of the three samples was obtained as the group OD value. The haemolysis ratio (HR) was expressed as the percentage and calculated according to the equation:

$$HR = (ODt - ODn)/(ODp - ODn) \times 100\%.$$

The ODt indicates the OD value of the tested group. The ODn and ODp are the OD values of the negative and positive control groups, respectively. Less than 5% haemolysis rate was regarded as a nontoxic effect level in this experiment.

2.9 Experimental lung metastasis assay

The tumour lung metastasis assay was established as previously described.[48] B16F10 cells were cultured with DMEM medium containing 10% FBS. After collection of the cells, the cells were resuspended with normal saline to the appropriate concentrations. Next, 0.2 mL of the B16F10 cells suspension (5 × 10^5 cells) was injected via the tail vein of the C57BL/6J mice. The animals were randomly divided into five groups, including the normal control, model control, positive control, PD high dose (6 mg/kg) and PD low dose (3 mg/kg) groups, 6 mice per group. Normal and model mice were administered with normal saline. The mice received cyclophosphamide (CTX, 20 mg/kg) as a positive control.[49] The successively intraperitoneal injection of drugs into the mice from the day after tumour inoculation and the body weights were monitored every two days. After 2 weeks of PD administration, the mice were sacrificed and the number of B16F10 colonies present on the surface of each group of lungs was determined by visual inspection using a stereoscopic dissecting microscope.

The lung tissue samples were fixed in neutral 10% formalin for 48 h and embedded in paraffin and sectioned (7 μm thickness) for histology. The sections were stained with haematoxylin and eosin (H&E) and examined using light microscopy (Nikon 90i, Nikon, Tokyo, Japan).

2.10 Tumor angiogenesis assay

Tumour angiogenesis was surveyed using male C57BL/6J mice, B16F10 cells (1×10^6) were injected intradermally into the ventral skin.[50] The animals were randomly divided into three groups, including the model control, PD high dose (6 mg/kg) and PD low dose groups (3 mg/kg). The model mice were administered with normal saline. After 10 days of successive intraperitoneal injection, the animals were sacrificed and the tumour was removed from the skin and imaged using a stereo microscope (Leica MZ95, Leica Instrument GmbH, Nussloch, Germany). The length of the tumour-directed vessels was analysed using the Image-ProPlus 6.0 software.

2.11 ELISA

The serum was collected before the mice were sacrificed and centrifuged twice at 4000 rpm for 10 min. The levels of IL-12, TNF-α, IFN-γ, MMP-2, and MMP-9 were determined using mouse enzyme-linked immunosorbent assay (ELISA) kits according to the manufacturer's instructions. The absorbance was measured at 450 nm in an ELISA reader (BioTek Epoch, BioTek, Winooski, VT, USA).

2.12 Statistical analyses

Statistical analyses were performed using SPSS 22.0 and GraphPad Prism 6.0. All data were expressed as the mean ± standard deviation (S.D). Data were analysed using ANOVA with the Tukey multiple comparisontest and Dunnett's multiple comparison test. Differences were considered significant if $p< 0.05$ and extremely significant if $p< 0.01$. All experiments performed *in vitro* were repeated three times. Statistical graphs were produced using GraphPad Prism 6.0.

3 Results

3.1 Effect of PD on the viability of B16F10 melanoma cells and HUVEC cells *in vitro*

In this study, the effect of PD on B16F10 and HUVECs cell viability was evaluated using MTT assay. B16F10 and HUVEC cells were exposed to various concentrations of PD for 24 h. The concentrations were 0, 10, 20, 40 and 80 μg/mL for B16F10 cells and 0, 5, 10, 20 and 40 μg/mL for HUVEC cells. These results showed that PD exhibited cellular toxicity in a concentration-dependent manner (Figure 2A and 2B).

3.2 Effect of PD on B16F10 melanoma cells adherence to HUVECs

The measurement of adherence was determined on the uptake of the Rose Bengal stain. As shown in Figure 2C, high concentrations of PD (20 and 40 μg/mL) strongly reduced the adhesive capacity of B16F10 cells. The number of adhesive cells was obviously decreased (20 and 40 μg/mL), and the inhibitory effect was at a low concentration of PD (5 and 10 μg/mL). Accordingly the inhibitory rates were 13.84, 17.55, 75.19, and 97.07%, respectively.

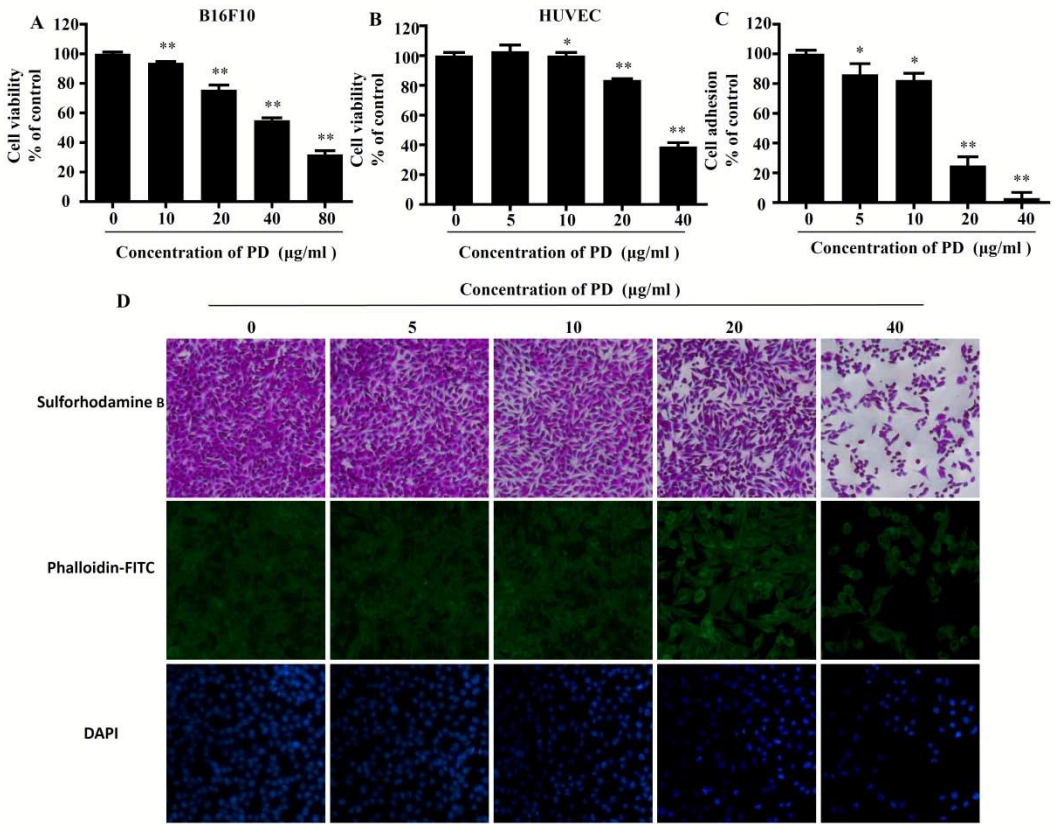

Fig.2 The effect of PD on cell viability, adhesion and morphological changes. (A) PD inhibited the viability of B16F10 cells in MTT assay. The results of the control were normalised to 100%, and the results from PD-treated cells were expressed as the % of control, $^{*}p$ <0.05, $^{**}p$ < 0.01. (B) PD inhibited the viability of HUVECs in the MTT assay. (C) PD showed inhibition effect on B16F10 cells adhered to HUVECs. (D) PD changed B16F10 cell morphology and actin cytoskeleton. B16F10 cells were stained with sulforhodamine B after cells were incubated with different concentrations of PD(magnification, ×200). Actin filaments were stained by FITC-conjugated phalloidinand (green). DAPI (blue) was applied to counter-stain the nucleus (magnification, ×400).

3.3 Effect of PD on the morphological characteristics of B16F10 cells

The ability of cells to form colonies is positively correlated with proliferation and metastatic potential. After exposure to PD for 24 h, as shown in (Figure 2D-sulforhodamine B), untreated B16F10 cells formed sizeable colonies and showed rapid proliferation. However, PD-treated B16F10 cells showed a reduced efficiency to form colonies.

To confirm the cellular morphological characteristics of PD, the change in the cytoskeletal organisation of B16F10 cells was further investigated. Fluorescent images were visualised using phalloidin-FITC staining (Figure 2D-phalloidin-FITC). DAPI (blue) was used to stain cell nuclei for clear observation. Figure 2D (green) showed a similar tendency as the sulforhodamine B staining assay. Normal control cells exhibited a normal cytoskeleton (green long bundles of stress fibres consisting of actin filaments). There was no significant difference between control cells and cells with low concentrations of PD (5, 10 μg/mL). However, PD (20, 40 μg/mL)-treated cells was confirmed to demonstrate less organised actin fibres. PD (20, 40 μg/mL) exhibited a significant decrease in the number of filopodia and lamellipodia compared to the number of PD-treated cells. Furthermore, PD treatment reduced filopodia and lamellipodia formation in a dose-dependent manner.

3.4 Effect of PD on migration of B16F10 melanoma cells

Effect of PD on cell migration was investigated using the wound-healing assay. We observed that B16F10 melanoma cells moved gradually from the edge of the wound to the blank area during the 24 h incubation, and the width of the wound in the PD-administered groups was wider than normal control. PD inhibited the migration of B16F10 melanoma cells in a concentration-dependent manner (Figure 3A).

3.5 Effect of PD on invasion of B16F10 melanoma cells

To investigate whether PD affects the invasion ability of B16F10 melanoma cells, an *in vitro* transwell invasion assay system was used. As shown in Figure 3B, the number of invaded B16F10 cells was decreased with an increase in PD concentration. The inhibitory rates of PD at 5, 10, 20, and 40 μg/mL were 25.24, 46.60, 57.28, and 75.73%, respectively.

3.6 Effect of PD on tube formation of HUVECs

To examine the effect of PD on crucial functions in blood vessel formation, we next investigated whether PD decreased the formation of tubes by HUVECs *in vitro*. Our results showed that PD remarkably inhibited HUVECs tube formation. Tube formation was imaged and length of the tubes was determined (Figure 3C). Treatment with PD resulted in 1.41, 14.84, 70.44, and 100% inhibition of tube formation at concentrations of 5, 10, 20, and 40 μg/mL, respectively.

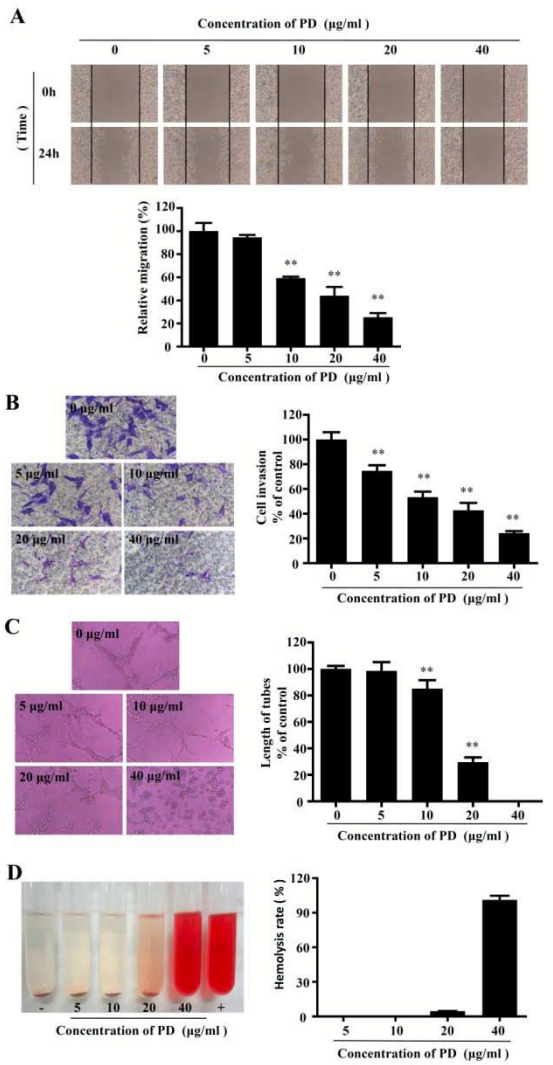

Fig3. The effect of PD on B16F10 metastasis and HUVECs tube formation *in vitro* combined with the haemolysis test. (A) PD showed an obvious inhibitory effect on B16F10 cells migration in the wound-healing assay. Based on the width of the wound at 0h, the relative width at 24h was calculated using Image-Pro Plus 6.0 software. (B) PD inhibited B16F10 cells invasion. The invaded cells were quantified and stained, and the relative invasion was quantified. (C) The HUVEC tubular structures were imaged under a microscope at ×200 magnification. Tube networks were quantified using Image-Pro Plus 6.0 software. $^{*}p$ <0 .05, $^{**}p$ < 0.01. (D) Haemolysis test results of various concentrations of PD.

3.7 Effect of PD on haemolysis test

Haemolysis rate is an important parameter for evaluating blood compatibility. Less than 5% haemolysis was regarded as a nontoxic effect level in this experiment.[51] Nearly no haemolysis was observed for the negative control (-) and complete haemolysis was observed for the positive control (+). The HR % of PD at different concentrations (5, 10, 20 μg/ml) was 0.06, 0.61, and 4.57%, respectively. The colour of the high concentration of PD group (40 μg/ml) turned red (Figure 3D) and the haemolysis rate was 101.11%. Thus, the results of the haemolysis test demonstrated that PD exhibited good biocompatibility under certain concentration (20 μg/mL) and can act as a promising platform for cancer treatment.

3.8 Effect of PD on B16F10 experimental lung metastasis.

Intraperitoneal injection of PD (3 and 6 mg/kg) for two weeks resulted in a significant decrease in the number of metastatic nodules on the lung surface compared to the model group (Figure 4A). The metastatic nodules on the lung surface were quantified (Figure 4B). These results showed that the weights of the lung were associated with the degree of tumour metastasis (Figure 4C). The number of lung metastasis nodules was 18.33 and 22.00 in mice administered with PD at 3 and 6 mg/kg, respectively. In the model and CTX control groups, the number was 125.67 and 13.67, respectively. This amount was decreased to a different extent in the CTX and PD treatment groups. The inhibitory rates of PD at 3 and 6 mg/kg on metastasis were 82.49 and 85.41%, respectively.

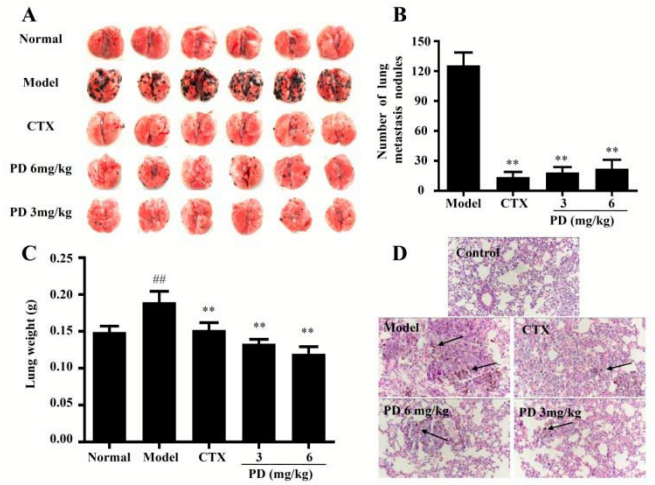

Fig. 4 The effect of PD on B16F10 melanoma cells experimental lung metastasis. B16F10 cells were injected into the tail vein of C57BL/6J mice. PD was administered with an intraperitoneal injection at 3 and 6 mg/kg for two weeks consecutively. Normal saline was administered to normal and model mice with the same schedule, and CTX was administered to positive mice. (A) After the mice were sacrificed, the lungs were excised, and metastatic nodules on the lung surface were imaged. (B) The metastatic nodules on the lung surface were quantified. (C) The lung weight was determined. (D) Histopathology of lung of metastatic B16F10-bearing animals (×200). Lungs were fixed in 10% neutral formalin after the mouse were sacrificed, 7 μm sections were obtained and stained with H&E, arrowheads indicate the metastatic foci.$^{\#\#}p < 0.01$ *vs* Normal, $^{**}p < 0.01$ *vs* Model.

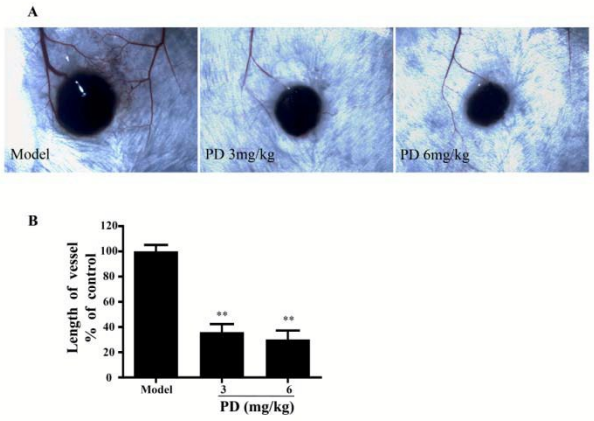

Fig. 5 PD suppressed tumour angiogenesis. (A) Peritumoural blood vessels were imaged under a microscope at × 6.3 magnification. Representative images of the mouse blood vessels directed to the tumor. (B) Length of the blood vessels was estimated using Image-Pro Plus 6.0 software. $^{**}p < 0.01$

The results from histological examination revealed the number of metastasis in lung sections of B16F10-bearing mice, while this number was dramatically reduced after CTX and PD treatment for two weeks (Figure 4D).

3.9 Effect of PD on tumour angiogenesis

C57BL/6J mice were used to evaluate the anti-angiogenesis effects of PD in B16F10 tumour-bearing mice. Ten days after successive intraperitoneal injection of PD, all mice showed well-developed tumours in the skin and the vessels were observed clearly (Figure 5A). The length of the peritumoural blood vessels were significantly reduced by treatment with PD (Figure 5B).

3.10 Effect of PD on cytokines and MMPs

To assess the effects of PD on cytokines and MMPs in the tumour microenvironment, an ELISA assay was performed to determine the serum levels of IL-12, TNF-α, IFN-γ and MMPs (Figure 6). Compared with the model group, the levels of IL-12and IFN-γ were significantly increased and the level of TNF-α was slightly elevated in the PD-treated group (p<0.05).These results indicated that PD may exert anti-metastasis effects by regulating these cytokines.

According to the serum levels of MMPs, we found that MMP-2 and MMP-9 consisted of a portion of factors involved in PD inhibition of tumour metastasis. The concentration of MMP-2 was 53.18, 61.58 and 101.88 ng/mL in the 3 mg/kg PD group, 6 mg/kg PD group, and model mice, respectively. The concentration of MMP-9 was 16.76, 18.78 and 36.13 ng/mL in the 3 mg/kg PD group, 6 mg/kg PD group, and model mice, respectively. ELISA data indicated that PD decreased the expression of both MMP-2 and MMP-9 compared to the model mice.

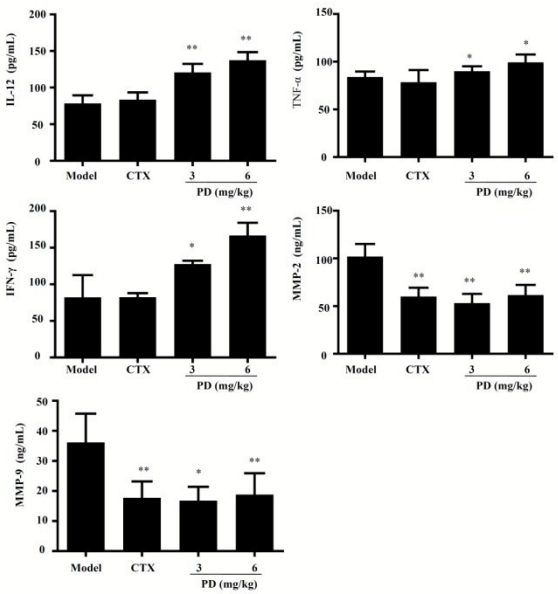

Fig.6 Effects of PD on the serum levels of cytokines and MMPs. The serum was collected after PD treatment for two weeks on B16F10-tumor bearing mice. The serum levels of IL-12, TNF-α, IFN-γ, MMP-2 and MMP-9 were measured using an ELISA assay. Data were presented as the mean ± SD, $^{**}p< 0.01$, $^{*}P< 0.05$.

4 Discussion

Cancer is a major public health problem worldwide. With respect to skin cancer, malignant melanoma is the most dangerous type of skin cancer; it is a highly metastatic cancer and has a poor prognosis once metastasis has occurred.[52] The recent increase in the prevalence of melanoma and the lack of effective treatments for metastatic disease make it one of the most devastating malignancies. Traditional treatments no longer meet the requirements for quality of life, particularly considering their serious poor bioavailability and side effects. Thus, development of novel agents and strategies for malignant melanoma metastasis is a priority and an important global medical issue. There is a need to explore new drugs to improve survival and quality of life.

PD, a natural agent extracted from *Platycodon grandiflorum*, exhibits a wide spectrum of pharmacological properties and has been shown to be a promising anticancer drug. In a previous study, PD has been confirmed to inhibit the proliferation and migration of various cancer cell lines *in vitro*. In the current study, visible metastasis inhibition in B16F10 melanoma after PD treatment was observed by experimental lung metastasis *in vivo*. This effect of PD is likely due to its anti-angiogenesis and anti-invasion activity. MTT assay results indicated that HUVECs are more sensitive to PD than B16F10 cells.

In addition, little difference was presented in mice between 3 and 6 mg/kg of PD group, but the antimetastasis and antiangiogenic activity of PD *in vitro* occurred in a concentration-dependent manner. A potential reason was that the mice received a relatively small dose (3 and 6mg/kg) of PD, and the metabolism of absorption and distribution presented little difference *in vivo*. Thus, low dose (3mg/kg) of PD was a best choice to treat malignant melanoma in this condition.

Tumour cell migration and invasion are critical steps in tumour progression and metastasis. Cell motility involves the formation of cell protrusions known as filopodia and lamellipodia. Such protrusions are known to play an important role in the machinery of cell movement as a result of actin polymerisation and cytoskeletal rearrangement. The filamentous actin (F-actin) cytoskeleton is a dynamic structure that is necessary for regulating cell functions such as cell motility, adhesion and internal architecture. The results showed that B16F10 cells exposed to PD may exhibit cytoskeletal disruption and cellular membrane dysfunction. The results revealed that PD dramatically inhibited the migration and invasion of B16F10 melanoma cells.

Angiogensis is an essential component of tumour metastasis. The present data proved that PD exhibited antiangiogenic activity via the tube formation assay *in vitro* and tumour angiogenesis *in vivo*. Haemolysis of the blood is an important problem associated with the bioincompatibility of materials. Haemolysis result means that PD will not lead to severe haemolysis at an appropriate dose.

Cytokines in the tumour microenvironment affect tumour growth and metastasis. IL-12 is an inflammatory cytokine that induces IFN-γ production from T lymphocytes and NK cells. It exhibits antitumor and antimetastatic biological effects.[53] In addition, IL-12 acts as an indirect inhibitor of angiogenesis.[54] TNF-α is a key cytokine in the tumour microenvironment involved in tumour progression.[55] IFN-γ is one such proinflammatory cytokine that plays an important role in immune responses to tumours, and it has pleiotropic effects in the tumour microenvironment, including the inhibition of cell proliferation and angiogenesis.[56] Both TNF-α and IFN-γ have been shown to affect blood vessel endothelial cells and inhibits proliferation and migration.[57] The present results showed that the serum levels of IL-12, TNF-α and IFN-γ were remarkably restored and enhanced after PD treatment compared with those in the model group. Interestingly, in splenocytes obtained from the HBsAg-immunised mice, PD could also significantly enhanced the concentration of cytokines IL-2 and IFN-γ.[18] In a previous study, PD exhibited the ability to modulate the secretion of TNF-α, and an increase in TNF-α production by PD treatment may stimulate TNF-α synthesis or inhibit the degradation of TNF-αmRNA.[58] Taken together, these data indicated that PD might increase the level of cytokines in the tumour microenvironment of B16F10 tumour-bearing mice by promoting cytokine release. The ability of cancer metastasis is related to the migration of cancer cells into and out of blood vessels to form a new metastatic colony. Angiogenesis is closely related to tumour metastasis and this process is related to the tumour microenvironment, and is mediated by cytokines and proteases MMPs. Particularly, MMP-2 and MMP-9, which play a vital role in the metastasis of cancer.[59, 60] MMPs mediate invasion and tumour metastasis by providing a mechanism through which tumour cells can traverse basement membranes, thereby gaining access to blood and lymphatic vessels. In the present study, CTX and PD significantly reduced the serum levels of MMP-2 and MMP-9 in B16F10-bearing mice. Coincidentally, following a tumour xenograft nude mice were administered of CTX, and the levels of

MMP-9 were significantly reduced compared with the control group.[61] We assumed that the effect of PD on MMP-2 and MMP-9 is responsible for the inhibitory activity of PD on B16F10 melanoma metastasis.

Conclusions

In conclusion, the present data demonstrated that PD inhibits the migration and invasion of B16F10 melanoma cells via anti-angiogenic activity. The findings in the present study indicate that PD has the potential to be an efficient anticancer drug in the treatment of metastatic malignant melanoma.

Conflicts of interest

The authors declare no conflict of interest.

Acknowledgements

This work was supported by the grants of National Natural Science Foundation of China (NO. 31201331), and of Jilin Science & Technology Development Plan (NO. 201201102, 20130303096YY, and 20150204050YY).

References

1 C. Vanessa, G. Schopfer, M. Karasarides, R. Hayward and R. Marais, *Cancer research*, 2007, **67**, 122-129.
2 R. Siegel, J. Ma, Z. Zou and A. Jemal, *CA: a cancer journal for clinicians*, 2014, **64**, 9-29.
3 E. M. Dunki-Jacobs, G. G. Callender and K. M. McMasters, *Current problems in surgery*, 2013, **50**, 351-382.
4 N. Wald and E. Goormaghtigh, *Analyst*, 2015, **140**, 2144-2155.
5 I.Tatsuaki, N. Motowo, N. Mikihiko, N. Tetswchiro and T. TakaShi, *Cancer research*, 1996, 875-879.
6 P. S. Steeg, *Nature medicine*, 2006, **12**, 895-904.
7 I. J. Fidler, *Nature Reviews Cancer*, 2003, **3**, 453-458.
8 B.R. Zetter, *Annual review of medicine*, 1998, **49**, 407-424.
9 J. Folkman, Journal of the National Cancer Institute, 1990, **82**, 4-7.
10 J. Folkman, *Nature medicine*, 1995, **1**, 27-30.
11 F. Eskens, *British journal of cancer*, 2004, **90**, 1-7.
12 J. Folkman, *Seminars in oncology,* 2002, **29**, 15-18.
13 J. B. Nair, S. Mohapatra, S. Ghosh and K. K. Maiti, *Chemical Communications*, 2015, **51**, 2403-2406.
14 C. Köppen, O. Reifschneider, I. Castanheira, M. Sperling, U. Karst and G. Ciarimboli, *Metallomics*, 2015, **7**, 1595-1603.
15 W. Li, X.-M. Su, Y. Han, Q. Xu, J. Zhang, Z. Wang and Y.-P. Wang, *RSC Advances*, 2015, **5**, 101850-101859.
16 W. A. Elmasri, M.-E. F. Hegazy, Y. Mechref and P. W. Paré, *RSC Advances*, 2015, **5**, 27126-27133.
17 A.P. Subramanian, A.A. John, M.V. Vellayappan, A. Balaji, S.K. Jaganathan, E. Supriyanto and M. Yusof, *RSC Advances*, 2015, **5**, 35608-35621.
18 A. Saha, S. Mohapatra, P. Kurkute, B. Jana, J. Sarkar, P. Mondal and S. Ghosh, *RSC Advances*, 2015, **5**, 92596-92601.
19 A. AlQathama and J.M. Prieto, *Natural Product Reports*, 2015, **32**, 1170-1182
20 X. Luan, Y.-G. Gao, Y.-Y. Guan, J.-R. Xu, Q. Lu, M. Zhao, Y.-R. Liu, H.-J. Liu, C. Fang and H.-Z. Chen, *Toxicology and applied pharmacology*, 2014, **281**, 118-124.
21 T. Chen, J. Gao, P. Xiang, Y. Chen, J. Ji, P. Xie, H. Wu, W. Xiao, Y. Wei and S. Wang, *International immunopharmacology*, 2015, **26**, 338-348.
22 L.-K. Han, Y.-N. Zheng, B.-J. Xu, H. Okuda and Y. Kimura, *The Journal of nutrition*, 2002, **132**, 2241-2245.
23 O. G. Kwon, S. K. Ku, H. D. An and Y. J. Lee, *Evidence-Based Complementary and Alternative Medicine*, 2014, **2014**. Article ID 954508.
24 T. Zhang, S. Yang, J. Du, Y. Jinfu and W. Shumin, *Inflammation*, 2015, **38**, 1221-1228.
25 S.-S. Choi, E.-J. Han, T.-H. Lee, J.-K. Lee, K.-J. Han, H.-K. Lee and H.-W. Suh, *Planta medica*, 2002, **68**, 794-798.
26 Y. Xie, H.-X. Sun and D. Li, *Vaccine*, 2009, **27**, 757-764.
27 J. Wu, G. Yang, W. Zhu, W. Wen, F. Zhang, J. Yuan and L. An, *Biological and Pharmaceutical Bulletin*, 2012, **35**, 1216-1221.
28 T. Li, W.-S. Xu, G.-S. Wu, X.-P. Chen, Y.-T. Wang and J.-J. Lu, *Asian Pac J Cancer Prev*, 2014, **15**, 1745-1749.
29 H. Qin, X. Du, Y. Zhang and R. Wang, *Tumor Biology*, 2014, **35**, 1267-1274.
30 J. C. Park, Y. J. Lee, H. Y. Choi, Y. K. Shin, J. D. Kim and S. K. Ku, *Evidence-Based Complementary and Alternative Medicine*, 2014, **2014**. Article ID 478653.
31 Y. S. Kim, J. S. Kim, S.-U. Choi, H. Lee, S. Roh, Y. Jeong, Y. Kim and S. Ryu, *Planta medica*, 2005, **71**, 566-568.
32 J. Chun, E. J. Joo, M. Kang and Y. S. Kim, *Journal of cellular biochemistry*, 2013, **114**, 456-470.
33 C. Xu, G. Sun, G. Yuan, R. Wang and X. Sun, *Molecules*, 2014, **19**, 21411-21423.
34 D. Y. Shin, G. Y. Kim, W. Li, B. T. Choi, N. D. Kim, H. S. Kang and Y. H. Choi, *Biomedicine & Pharmacotherapy*, 2009, **63**, 86-94.
35 M. O. Kim, D. O. Moon, Y. H. Choi, J. D. Lee, N. D. Kim and G. Y. Kim, *International journal of cancer*, 2008, **122**, 2674-2681.
36 J. S. Yu and A. K. Kim, *Journal of medicinal food*, 2010, **13**, 298-305.
37 Z.-H. Tang, T. Li, H.-W. Gao, W. Sun, X.-P. Chen, Y.-T. Wang and J.-J. Lu, *Chinese medicine*, 2014, **9**, 16.
38 T. Li, Z.-H. Tang, W.-S. Xu, G.-S. Wu, Y.-F. Wang, L.-L. Chang, H. Zhu, X.-P. Chen, Y.-T. Wang, Y. Chen and J. –J. Lu, *European journal of pharmacology*, 2015, **749**, 81-88.
39 J. Chun and Y. S. Kim, *Chemico-biological interactions*, 2013, **205**, 212-221.
40 W. Li, Y. Liu, Z. Wang, Y. Han, Y. H. Tian, G. S. Zhang, Y. S. Sun and Y. P. Wang, *Food & function*, 2015, **6**, 1418-1427.
41 F. Li, S. Li, H.-B. Li, G.-F. Deng, W.-H. Ling and X.-R. Xu, *Food & function*, 2013, **4**, 530-538.
42 C.-C. Liang, A. Y. Park and J.-L. Guan, *Nature protocols*, 2007, **2**, 329-333.
43 W. Zhang, B. Tang, Q. Huang and Z. Hua, *Journal of cellular biochemistry*, 2013, **114**, 152-161.

44 M. Donà, I. Dell'Aica, E. Pezzato, L. Sartor, F. Calabrese, M. Della Barbera, A. Donella-Deana, G. Appendino, A. Borsarini and R. Caniato, *Cancer research*, 2004, **64**, 6225-6232.
45 O. P. Barry, D. Praticò, R. C. Savani, FitzGerald and GA, *Journal of Clinical Investigation*, 1998, **102**, 136-144.
46 P. Y. Yue, D. Y. Wong, P. Wu, P. Leung, N. Mak, H. Yeung, L. Liu, Z. Cai, Z.-H. Jiang and T. Fan, *Biochemical pharmacology*, 2006, **72**, 437-445.
47 C. Li, J. Jin, J. Liu, X. Xu and J. Yin, *RSC Advances*, 2014, **4**, 24842-24851.
48 I. J. Fidler, *Cancer research*, 1975, **35**, 218-224.
49 L. Lu, F. Payvandi, L. Wu, L.-H. Zhang, R. J. Hariri, H.-W. Man, R. S. Chen, G. W. Muller, C. C. Hughes and D. I. Stirling, *Microvascular research*, 2009, **77**, 78-86.
50 F. Seguin, M. Carvalho, D. Bastos, M. Agostini, K. Zecchin, M. Alvarez-Flores, A. Chudzinski-Tavassi, R. Coletta and E. Graner, *British journal of cancer*, 2012, **107**, 977-987.
51 Q. Du, C. Fu, J. Tie, T. Liu, L. Li, X. Ren, Z. Huang, H. Liu, F. Tang, L. Li and X. Meng, *Nanoscale*, 2015, **7**, 3147-3154.
52 P.-D. Duh, Z.-T. Chen, S.-W. Lee, T.-P. Lin, Y.-T. Wang, W.-J. Yen, L.-F. Kuo and H.-L. Chu, *Journal of agricultural and food chemistry*, 2012, **60**, 7866-7872.
53 J. Hendrzak and M. Brunda, in *Attempts to Understand Metastasis Formation III*, Springer, 1996,**213/3**, 65-83.
54 E. E. Voest, B. M. Kenyon, M. S. O'Reilly, G. Truitt, R. J. D'Amato and J. Folkman, *Journal of the National Cancer Institute*, 1995, **87**, 581-586.
55 F. Balkwill, *Nature Reviews Cancer*, 2009, **9**, 361-371.
56 U. Boehm, T. Klamp, M. Groot and J. Howard, *Annual review of immunology*, 1997, **15**, 749-795.
57 N. Sato, H. Nariuchi, N. Tsuruoka, T. Nishihara, J. G. Beitz, P. Calabresi and A. R. Frackelton, *Journal of Investigative Dermatology*, 1990, **95**, 85S-89S.
58 C. Wang, G. B. S. Levis, E. B. Lee, W. R. Levis, D. W. Lee, B. S. Kim, S. Y. Park and E. Park, *International immunopharmacology*, 2004, **4**, 1039-1049.
59 E. I. Deryugina and J. P. Quigley, *Cancer and Metastasis Reviews*, 2006, **25**, 9-34.
60 M. Egeblad and Z. Werb, *Nature Reviews Cancer*, 2002, **2**, 161-174.
61 Z. Sun, T. Yzu, J. Chen, X. Sun, F. Gao, X. Zhao and J. Luo, *Journal of International Medical Research*, 2010, **38**, 967-976.

Platycodin D inhibits B16F10 melanoma metastasis via antiangiogenic activity

Platycodon grandiflorum

extract

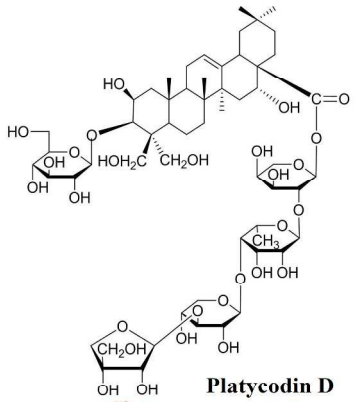

Platycodin D